

## THE ASSEMBLY OF GALAXY CLUSTERS

JOEL C. BERRIER, KYLE R. STEWART, JAMES S. BULLOCK, CHRIS W. PURCELL, ELIZABETH J. BARTON  
Center for Cosmology, Department of Physics and Astronomy, The University of California at Irvine, Irvine, CA 92697, USA

RISA H. WECHSLER

Kavli Institute for Particle Astrophysics and Cosmology, Physics Department, and Stanford Linear Accelerator Center, Stanford University,  
Stanford, CA 94305, USA  
*Draft version April 2, 2008*

## ABSTRACT

We study the formation of fifty-three galaxy cluster-size dark matter halos ( $M = 10^{14.0-14.76} M_{\odot}$ ) formed within a pair of cosmological  $\Lambda$ CDM N-body simulations, and track the accretion histories of cluster subhalos with masses large enough to host  $\sim 0.1L_{*}$  galaxies. By associating subhalos with cluster galaxies, we find the majority of galaxies in clusters experience no “pre-processing” in the group environment prior to their accretion into the cluster. On average,  $\sim 70\%$  of cluster galaxies fall into the cluster potential directly from the field, with no luminous companions in their host halos at the time of accretion; and less than  $\sim 12\%$  are accreted as members of groups with five or more galaxies. Moreover, we find that cluster galaxies are significantly less likely to have experienced a merger in the recent past ( $\lesssim 6$  Gyr) than a field halo of the same mass. These results suggest that local, cluster processes like ram-pressure stripping, galaxy harassment, or strangulation play the dominant role in explaining the difference between cluster and field populations at a fixed stellar mass; and that pre-evolution or past merging in the group environment is of secondary importance for setting cluster galaxy properties for most clusters. The accretion times for  $z = 0$  cluster members are quite extended, with  $\sim 20\%$  incorporated into the cluster halo more than 7 Gyr ago and  $\sim 20\%$  within the last 2 Gyr. By comparing the observed morphological fractions in cluster and field populations, we estimate an approximate timescale for late-type to early-type transformation within the cluster environment to be  $\sim 6$  Gyr.

*Subject headings:* cosmology: theory, large-scale structure of universe — galaxies: formation, evolution, high-redshift, interactions, statistics

## 1. INTRODUCTION

Galaxy clusters are over-abundant in red, early-type galaxies compared to the field population (Oemler 1974; Butcher & Oemler 1978; Dressler 1980; Dressler et al. 1997; Treu et al. 2003; Balogh et al. 2004; Poggianti et al. 2006; Capak et al. 2007). Approximately 60% of bright galaxies located within the virial radii of cluster halos are bulge-dominated (E + S0) compared to  $\sim 30\%$  of similar luminosity galaxies located in very low-density environments (Whitmore & Gilmore 1991; Postman et al. 2005). The fraction of weakly star-forming, early-type galaxies grows with the local galactic density, but even poor groups show differences compared to the general population (e.g., Postman & Geller 1984; Dressler et al. 1997; Zabludoff & Mulchaey 1998; Tran et al. 2001; Finn et al. 2008).

One suggestion is that “pre-processing” in the group environment prior to cluster formation is important in setting the early-type fraction in clusters (e.g., Zabludoff & Mulchaey 1998; Zabludoff 2002). A related possibility is that galaxies in clusters typically experience more mergers than field galaxies (prior to their accretion), and that this merger history bias plays a role in explaining population differences (Toomre & Toomre 1972). Finally, the fact that the overall mix of galaxies in clusters by type is known to evolve with redshift (Butcher & Oemler 1978; Ellingson et al. 2001; Tran et al. 2005; Gerke et al. 2007; Capak et al. 2007; Coil et al. 2008; Loh et al. 2008; Finn et al. 2008) suggests that the internal cluster processes play a major role in setting the differences between the cluster and field populations.

Here we examine the formation of clusters in a  $\Lambda$ CDM cosmological simulation in order to gain insight into these questions.

Galaxies in clusters and groups are subject to a number of processes that may suppress star formation or change the morphology of a galaxy. One such effect, ram-pressure stripping (Gunn & Gott 1972; Quilis et al. 2000) seems to have been observed directly in Virgo (Chung et al. 2007), and simulations suggest that this process should operate on short,  $\sim 1$  Gyr, timescales (Tonnesen 2007). Other processes of relevance include galaxy-galaxy “harassment” within the cluster potential (Moore et al. 1996) and cold gas “strangulation” (Larson et al. 1980; Kauffmann et al. 1993), which cuts off the gas supply for ongoing star formation in cluster galaxies.

By incorporating subsets of these expected cluster processes into semi-analytic plus N-body models, several groups have investigated cluster galaxy population trends in the context of  $\Lambda$ CDM (Balogh et al. 2000; Benson et al. 2001; Diaferio et al. 2001; Okamoto & Nagashima 2001; Springel et al. 2001). Broadly speaking, these models have been successful in producing the general behavior that early type galaxies are more common in clusters, but full agreement between theory and observation has yet to be achieved. This is likely because some of the relevant processes (e.g., ram pressure stripping, harassment) have been neglected, and perhaps because some of the effects that were included (e.g., morphological transformation via mergers) were modeled by rough approximations. Our approach is related to these past theoretical efforts, but different in its goal. Specifically, we aim to quantify the basic assembly statistics for cluster member halos using N-body simulations and to present these as a

basis for evaluating scenarios and interpreting observations. Surely, many of the of the statistical results presented here were implicitly included in past theoretical models that used N-body simulations as a basis, but our aim is to present the  $\Lambda$ CDM predictions as purely as possible, without obscuring them with any particular set of model assumptions for the baryon physics.

In what follows we use a pair of N-body simulations to track the assembly history of cluster-size dark matter halos. In section § 2 we discuss the simulations and the method for finding halos and subhalos. We present our findings in § 3. We reserve § 4 for a discussion of potential implications. We conclude in § 5.

## 2. METHODS

We study the formation histories of fifty-three  $M > 10^{14}h^{-1}M_{\odot}$  cluster-size dark matter halos extracted from two cosmological N-body simulations with comoving cubic volumes of  $120h^{-1}\text{Mpc}$  and  $80h^{-1}\text{Mpc}$  on a side. Each simulation corresponds to a flat  $\Lambda$ CDM cosmology with  $\Omega_{\text{M}} = 1 - \Omega_{\Lambda} = 0.3$ ,  $h = 0.7$ , and  $\sigma_8 = 0.9$  and were performed using the Adaptive Refinement Tree (ART) code of Kravtsov et al. (1997). As discussed in Allgood et al. (2006) and Wechsler et al. (2006), the  $80h^{-1}\text{Mpc}$  simulation followed the evolution of  $512^3$  particles with a mass of  $3.18 \times 10^8 h^{-1}M_{\odot}$  and achieved a maximum force resolution of  $1.2h^{-1}\text{kpc}$ . The  $120h^{-1}\text{Mpc}$  simulation (Allgood et al. 2006) followed the evolution of  $512^3$  particles with a mass of  $1.07 \times 10^9 h^{-1}M_{\odot}$  with a maximum force resolution of  $1.8h^{-1}\text{kpc}$ .

We identify halos in the simulation using a variation of the Bound Density Maxima Algorithm (BDM Klypin et al. 1999), specifically adopting the methods outlined in Kravtsov et al. (2004). As described in Stewart et al. (2008), virial radii and virial masses for halos are set by the radius within which the average density is  $\Delta_{\text{vir}}$  times the mean density of the universe (e.g., Bryan & Norman 1998). At  $z = 0$  this definition implies a radius-mass relation of  $R_{\text{vir}} \simeq 951(M_{\text{vir}}/10^{14}h^{-1}M_{\odot})^{1/3}$ . *Subhalos* are defined to be self-bound halos with centers located within the radius of a larger halo. In most cases, subhalo density profiles become overwhelmed by the larger halo’s density field at a truncation radius,  $R_t$ , that is smaller than  $R_{\text{vir}}$ . The truncation radius is defined to be the radius where a halo’s density profile flattens to a value larger than  $-0.5$ . We define a halo’s mass,  $M$ , to be the minimum  $M_{\text{vir}}$  and the mass within  $R_t$ .

We use 48 snapshot outputs from the  $80h^{-1}\text{Mpc}$  simulation, spaced roughly equally in expansion factor  $a = 1/(1+z)$  back to  $z = 21.6$  to generate merger histories for halos and subhalos. For the  $120h^{-1}\text{Mpc}$  simulation we used 91 snapshot outputs, spaced roughly equally in expansion factor back to a  $z = 10.1$ . The merger trees were derived using the methods discussed in Allgood et al. (2006), Wechsler et al. (2006), and Stewart et al. (2008). When halos are accreted into larger halos, we record the mass at this time and label it  $M_{\text{in}}$ . For halos that are not subhalos (field halos) we set  $M_{\text{in}} = M$ . We use this mass,  $M_{\text{in}}$ , as a proxy for luminosity in defining our cluster galaxy samples (see below). Once a halo becomes a subhalo, we continue to track its mass as it evolves within the larger halo. When subhalos fall below a critical mass,  $M_{\text{cr}} < M_{\text{in}}$ , we explicitly remove them from our catalogs, and assume that any galaxy it was hosting has fallen out of the observational sample (either because it has lost a significant fraction of luminous mass or because it has been disrupted). This choice for  $M_{\text{cr}}$  allows us to define a sample cleanly at a mass scale

where our halo finder is complete and our simulations are not strongly affected by over-merging.

In what follows we will assume that halos and subhalos with  $M_{\text{in}}$  larger than a specific threshold will host one galaxy at their center. If a halo contains one or more subhalos, it is assigned one “central” galaxy in addition to one galaxy for each of its subhalos. The term *host* is used to describe the largest halo that contains a galaxy. A halo need not contain a subhalo in order for it to be classified as a *host*, it simply needs to be massive enough to contain a galaxy at its center. A subhalo cannot be a host. Finally, we term *field* halos to be all halos that are not contained within a larger halo. Thus, by definition field halos cannot be subhalos.

By associating galaxies with subhalos larger than a critical mass *at the time of their accretion*, we are adopting a strategy similar to that used successfully by Conroy et al. (2006) and Berrier et al. (2006). These authors were able to reproduce both the large-scale and small-scale clustering statistics of galaxies by assuming a monotonic relationship between the luminosity of a galaxy and the maximum circular velocity that its halo had when it is first accreted into a larger halo (see Wang et al. 2006, for a similar approach).

Our primary population of cluster galaxies is defined by setting  $M_{\text{in}} > 10^{11.5}$  and  $M_{\text{cr}} > 10^{11.0}h^{-1}M_{\odot}$ . Averaging over both simulation volumes, this choice defines a sample with number density  $n_g = 0.012h^3\text{Mpc}^{-3}$ . Matching this number density to the Sloan Digital Sky Survey (SDSS) r-band luminosity function (Blanton et al. 2003), we estimate that these cuts correspond to a galaxy population with an r-band magnitude brighter than  $M_r \simeq -18.5$  for  $h = 0.7$ . This is comparable to the luminosity ranges used in most cluster morphology studies (e.g., Dressler 1980; Dressler et al. 1997; Postman et al. 2005). Note that our results are insensitive to the precise choice of  $M_{\text{cr}}$ . We have redone the analysis described below and using an  $M_{\text{cr}}$  value that differs by a factor of  $\sim 3$  from our fiducial  $M_{\text{cr}}$  and find virtually identical results.

Twelve of our cluster halos are taken from the higher resolution  $80h^{-1}\text{Mpc}$  simulation. For these high-resolution clusters, we explore the accretion histories of a second set of lower-mass cluster subhalos with  $M_{\text{in}} > 10^{11.0}$  and  $M_{\text{cr}} > 10^{10.3}h^{-1}M_{\odot}$ . This sample has a number density of  $n_g = 0.042h^3\text{Mpc}^{-3}$ , which, with  $h = 0.7$ , corresponds to minimum luminosity of  $M_r \simeq -16.4$  using the SDSS luminosity function (Blanton et al. 2003). This sample will be used to test the dependence of our results on sample selection and should represent galaxies that are comparable to (although somewhat fainter than) the observational sample studied by Treu et al. (2003).

Of course, these estimated cluster galaxy luminosities are only approximate. We certainly don’t expect that a simple mapping between mass and luminosity will hold in detail, especially within the cluster environment. However, as we show below, our results do not depend strongly on the adopted mass cut. This suggests that the uncertain mapping between individual halo masses their associated galaxy luminosities should not hinder the interpretation of our results.

The total sample of 53 cluster halos have  $z = 0$  masses spanning  $M_{\text{clus}} = (1.0 - 5.8) \times 10^{14}h^{-1}M_{\odot}$ , with a median mass of  $1.48 \times 10^{14}h^{-1}M_{\odot}$ . The total number of galaxy subhalos in this, our main sample of  $M_{\text{in}} > 10^{11.5}h^{-1}M_{\odot}$  subhalos is 834 ( $\sim 15$  per cluster). We also explore trends with cluster halo mass by dividing our main cluster sample into three mass bins

containing 18, 17, and 18 clusters each, with mass ranges that span  $10^{14.0-14.13}$ ,  $10^{14.13-14.24}$ , and  $10^{14.24-14.76} h^{-1} M_{\odot}$ , respectively. The clusters in these respective samples contain an average of  $\sim 9$ ,  $\sim 14$ , and  $\sim 25$  galaxies each. The subset of 12 high-resolution cluster halos we study have  $z = 0$  masses that span  $M_{\text{clus}} = (1.0-3.4) \times 10^{14} h^{-1} M_{\odot}$ . These clusters host a total of 643 subhalos that meet our  $M_{\text{in}} > 10^{11.0} h^{-1} M_{\odot}$  criterion and have an average of  $\sim 54$  galaxies per cluster. The most massive cluster in this sample hosts 102 galaxies. A summary of the clusters we study along with some properties of their accretion histories are given in Table 1.

In order to investigate the assembly of more massive clusters we also study clusters generated semi-analytically using the code described in Zentner et al. (2005, see also Zentner & Bullock 2003). This model uses the extended Press-Schechter (EPS) formalism, applying the specific implementation of Somerville & Kolatt (1999) to produce mass accretion histories for host halos of a given present-day mass, and then tracks the orbital evolution of each tree’s subhalos in their host potential via analytic prescriptions governing dynamical friction and tidal mass loss. The initial orbital energy and impact parameter for each satellite system are drawn from probability distributions yielded by cosmological N-body simulations. This algorithm produces several statistics which match those produced in well understood cosmological simulations. While not as accurate as our numerical simulations, this computationally-inexpensive semi-analytic model allows us to explore trends with cluster mass (from  $10^{13} h^{-1} M_{\odot} \leq M_{\text{clus}} \leq 10^{15.3} h^{-1} M_{\odot}$ ) with thousands of stochastically-generated halo formation histories.

### 3. RESULTS

#### 3.1. The environmental history of cluster galaxies

Before presenting results on the characteristics of cluster galaxies, we first explore the *mass* assembly distribution for the clusters themselves. The solid, monotonically increasing line in Figure 1 shows the mass fraction of our  $z = 0$  sample of 53 clusters that was built up from accreting halos more massive than  $M$ , where  $M$  is the halo mass just prior to accretion into the cluster. Note that we have normalized the accreted halo mass  $M$  relative to the final cluster mass at  $z = 0$ ,  $M/M_{\text{clus}}$ . The histogram shows the corresponding differential distribution. We see that the distribution peaks at  $M/M_{\text{clus}} \sim 0.1$ . This result is consistent with the expectation that dark matter halos of any size mass are built primarily from objects that are  $\sim 10\%$  of the mass of the final halo (Purcell et al. 2007; Stewart et al. 2008; Zentner 2007). Note that more than half of the mass accreted from objects large enough to host galaxies ( $M/M_{\text{clus}} \gtrsim 0.001 M_{\text{clus}}$ ) is accreted from group-scale systems with  $M/M_{\text{clus}} \gtrsim 0.1 M_{\text{clus}}$ .

Compare this result to Figure 2, which shows the fraction of  $z = 0$  cluster *galaxies* that were accreted as members of host halos of a given mass. The short-dashed (blue), solid (black) and long-dashed (red) lines correspond to clusters in our three mass bins, centered on  $z = 0$  masses  $M_{\text{clus}} \simeq 10^{14.05}$ ,  $10^{14.2}$ , and  $10^{14.35} h^{-1} M_{\odot}$ , respectively. We see that for the typical cluster in our sample, only  $\sim 25\%$  of the cluster’s galaxies were accreted as part of group-size objects with  $M > 10^{13} h^{-1} M_{\odot}$ . For the lowest and highest mass subsamples we see that  $\sim 15\%$  and  $\sim 30\%$  of galaxies are accreted from group-mass halos. The results are not sensitive to the selection of our  $M_{\text{cr}}$  value.

The previous two figures show that cluster *mass* assembly is dominated by the most massive (group-size) accretion events, while cluster *galaxy* assembly is dominated by lower-mass

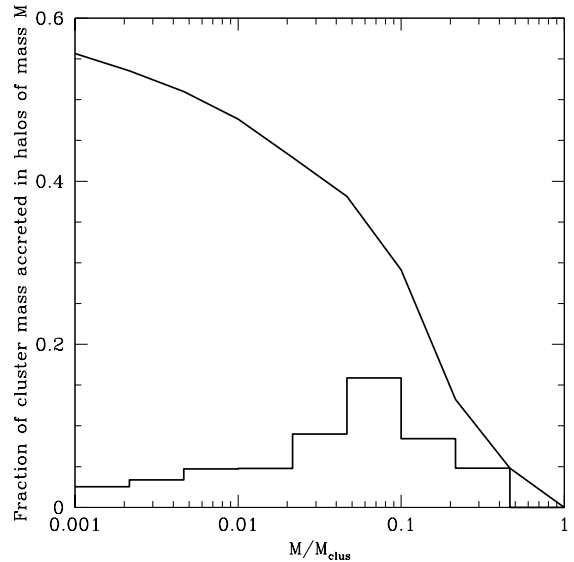


FIG. 1.— Cumulative and differential fraction of cluster mass,  $M_{\text{clus}}$ , accreted in halos of mass  $M/M_{\text{clus}}$  over the history of the simulation. This is an average result based on our sample of 53 clusters with a typical mass of  $M_{\text{clus}} \simeq 10^{14.2} h^{-1} M_{\odot}$ .

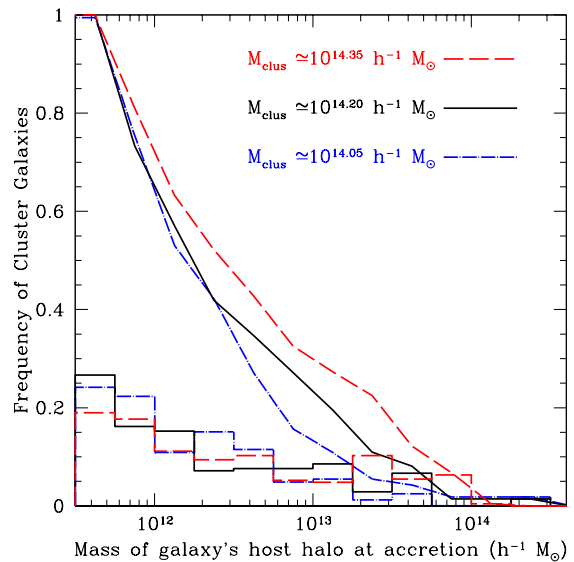


FIG. 2.— Cumulative and differential fraction cluster galaxies that fell into their respective clusters as part of a host halo of a given mass. Cluster galaxies were identified with  $M_{\text{in}} \geq 10^{11.5} h^{-1} M_{\odot}$ , corresponding to galaxies brighter than  $M_r \approx -18.5$ . The red-dash, black-solid, and blue-dot-dash lines correspond to increasing cluster halo mass bins, as labeled. The lines that increase monotonically towards lower accreted halo masses are the same distributions presented cumulatively.

(galaxy-size) halos. This can be understood by noting that the number of galaxies that a halo hosts does not increase linearly with host mass. A small group ( $M \sim 10^{12.5} h^{-1} M_{\odot}$ ) contains  $\sim 10$  times the mass of a single-galaxy halo ( $M \sim 10^{11.5} h^{-1} M_{\odot}$ ). However, typically a group halo of this mass will host only  $\sim 2-3$  galaxies that are as bright as the galaxies associated with  $10^{11.5} h^{-1} M_{\odot}$  halos. (e.g., Berrier et al. 2006, and references therein). This means that a small number of group-size halos can deposit a significant amount of mass into a cluster without contributing an equally large fraction of its galaxies.

While the mass of a galaxy’s host at accretion provides some insight into the environment within which it formed and

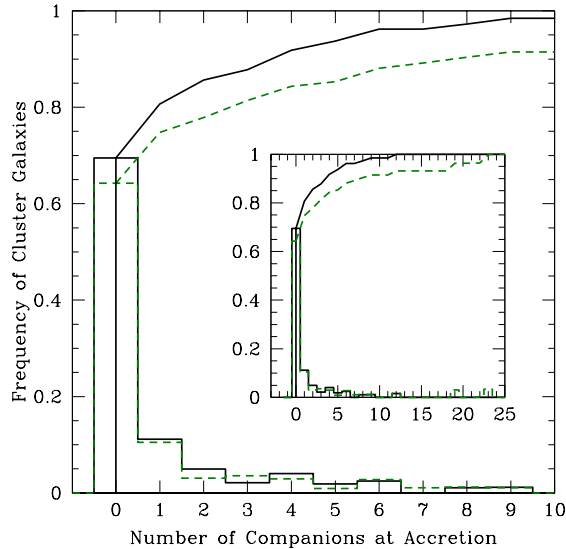


FIG. 3.— The fraction of surviving cluster galaxies,  $N_g/N_{\text{total}}$ , that fell into their clusters along with a given number of companions in their host dark matter halo. The black solid line corresponds to our standard galaxy sample ( $M_r \lesssim -18.5$ ) while the green dashed line shows the same distribution for our high resolution sample ( $M_{\text{in}} \geq 10^{11} h^{-1} M_{\odot}$ ,  $M_r \lesssim -16.4$ ). The inset box shows the distribution out to the maximum number of companions found in our sample in order to illustrate the tail of the distribution. Note that “companions” do not have to survive in order to be included in the count. We see that, on average,  $\sim 70\%$  of cluster galaxies fell into their clusters directly from the “field” (with zero companions in their dark matter halos), while  $\sim 80\%$  fell in with 2 or fewer companions.

evolved before joining the cluster, a more direct measure of the environment can be obtained by counting the number of galaxies that each host halo contained at the time of its infall. Figure 3 shows the distribution of the number of *companions* each cluster galaxy had within its host halo at the time it was accreted into the cluster. The companion count includes any other galaxies that existed within a galaxy’s host halo at the time of accretion. We do not require that a companion galaxy “survives” with  $M > M_{\text{cr}}$  at  $z = 0$  in order to include it in this count — it simply must have  $M > M_{\text{cr}}$  at the time of accretion into the cluster. A companion count of zero implies that the galaxy was accreted as the only object in its halo (*i.e.*, it was accreted from the field). The two solid lines show the binned and cumulative distributions for our standard sample of 834 galaxies within 53 clusters, and the pair of dark green dashed lines correspond to our sample of 643 lower mass galaxy halos taken from the 12 high-resolution clusters. For our standard sample, approximately 70% of cluster galaxies were accreted as the only galaxy within their halo and  $\sim 88\%$  were accreted with fewer than 5 galaxies. The numbers are similar for the sample that includes smaller galaxy halos. In this case,  $\sim 65\%$  of the cluster galaxies are accreted directly from the field.

So far we have considered only *averages* for entire samples and sub-samples of our cluster-galaxy population. We would also like to obtain some indication of the variation in assembly histories from cluster to cluster. Figure 4 presents statistics on the individual ( $M_{\text{in}} > 10^{11.5} h^{-1} M_{\odot}$ ) galaxy populations subdivided into their respective clusters. The red-dashed line shows the distribution of our clusters that have a given fraction ( $f$ ) of their galaxies accreted directly from the “field”, as the only object in their halos. For example, an abscissa value of  $f = 0.5$  implies that 50 % of a cluster’s

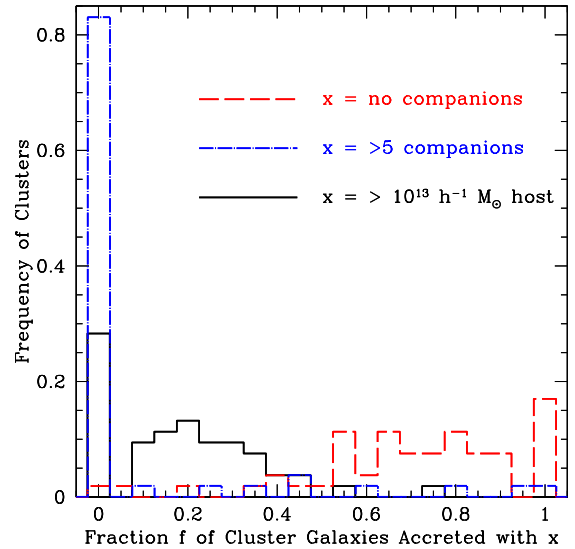


FIG. 4.— Distribution of galaxy clusters with a given assembly history. The red-dashed line shows the frequency of simulated clusters that have a given fraction  $f$  of their galaxies accreted directly from the field (with no companions in their host halos as they fell in,  $f = N_0/N_{\text{total}}$ ). The red-dashed peak at  $f = 1$  shows that  $\sim 18\%$  of our clusters have had 100% of their galaxies accreted directly from the field. The blue-dot-dashed line shows the frequency of clusters with a given fraction of their galaxies accreted with five or more companions in their host halos ( $f = N_{>5}/N_{\text{total}}$ ). The large peak at  $f = 0$  shows that  $\sim 83\%$  of our simulated clusters have had none of their galaxies accreted from groups with five or more companions. Finally, the solid line shows the frequency of simulated clusters with a given fraction of their galaxies that were accreted as part of a group-mass halo with  $M > 10^{13} h^{-1} M_{\odot}$ . The broad bump around  $f \sim 0.2$  shows that, typically, our clusters have  $\sim 10\text{--}40\%$  of their galaxies accreted from halos larger than the  $\sim 10^{13} h^{-1} M_{\odot}$ . Here we used our standard galaxy sample with  $M_{\text{in}} \geq 10^{11.5} h^{-1} M_{\odot}$ ,  $M_r \lesssim -18.5$ .

galaxies were accreted from the field. The peak in the red-dashed histogram at  $f = 1$  shows that  $\sim 18\%$  (10/53) of our clusters were assembled entirely from field accretions. The blue, short-dashed line shows the distribution of our clusters that had a fraction  $f$  of their galaxies accreted together with 5 or more companions in their host halos at the time of their infall into the cluster. The spike in the blue short-dashed histogram at  $f = 0$  implies that  $\sim 83\%$  (44/53) of our clusters had none of their galaxies accreted from a group with 5 or more companions. Finally, the solid line shows the frequency of clusters with a fraction  $f$  of their galaxies accreted from within group-mass halos with  $M \geq 10^{13} h^{-1} M_{\odot}$ . We see that most clusters have between  $f = 10\%$  and  $40\%$  of their galaxies accreted from group-mass halos. However, the solid-line’s peak at  $f = 0$  shows that a non-negligible fraction ( $\sim 28\%$ , 15/53) of our clusters had none of their galaxies accreted as members of group or cluster-size halos.

### 3.2. Trends with Cluster Mass

Figure 2 shows that more massive clusters are more likely to have had their galaxies accreted from massive host halos. Figure 5 explores the issue of mass dependence more fully. Shown is the fraction of surviving cluster galaxies that fell into the cluster without a bright companion in their host halo at the time of accretion as a function of the cluster mass. The three triangle data points show the median fractions for three mass bins based on our standard sample of 53 clusters with galaxy halos set via  $M_{\text{in}} > 10^{11.5} h^{-1} M_{\odot}$ ,  $M_r \lesssim -18.5$ . The square data point is from our high-resolution sample, with galaxies identified using our  $M_{\text{in}} > 10^{11} h^{-1} M_{\odot}$  criterion, cor-

responding to  $M_r \lesssim -16.4$ . Vertical error bars correspond to the sixty-eighth percentile range and the horizontal error bars span the mass range of clusters included in the bins. As expected, we do see a slight mass trend in the median, with the fraction of field-accreted galaxies falling from  $\sim 75\%$  to  $\sim 65\%$  as the cluster mass increases from  $\sim 10^{14} h^{-1} M_\odot$  to  $\sim 3 \times 10^{14} h^{-1} M_\odot$ , although the overall trend is weak compared to the scatter from cluster-to-cluster at fixed mass.

In order to explore how this trend continues over a broader cluster mass range, we have used the Zentner et al. (2005) semi-analytic merger-tree and substructure code (see also, Purcell et al. 2007) to generate 1000 cluster halo realizations at each of 10 cluster halo mass values between  $M_{\text{clus}} = 10^{13}$  and  $2 \times 10^{15} h^{-1} M_\odot$ . The three line types correspond to three different choices for defining the galaxy samples, with  $M_{\text{in}} > 10^{12}$ ,  $10^{11.5}$ , and  $10^{11} h^{-1} M_\odot$ , from top-to bottom, respectively. Galaxy subhalos are counted at  $z=0$  as surviving galaxies if they maintain masses larger than  $M_{\text{cr}} = 10^{11}$ ,  $10^{11}$ , and  $10^{10.5} h^{-1} M_\odot$ , respectively. The long-dashed red and solid black lines should correspond to the red triangle and black square N-body points, respectively. While the overall normalization of the semi-analytic estimates is low compared to the N-body result, the mass trend is in approximate agreement, with more massive clusters accreting a smaller fraction of their galaxies directly from the field, with a mass scaling as  $\sim M_{\text{clus}}^{-0.2}$  over the mass range plotted. Note that we expect even the most massive clusters to have a significant fraction of their galaxies accreted directly from the field.

### 3.3. Cluster assembly with time

The results presented in the previous section suggest that most cluster galaxies experienced no evolution in a group environment prior to their accretion into the cluster, lending support to the idea that internal cluster processes are responsible for the differences seen between cluster galaxies and those in field environments. If this is so, then the distribution of time spent in the cluster environment can provide insight into the timescales required for morphological transformation or the truncation of star formation.

Figure 6 shows the distribution of accretion times for surviving cluster galaxies in our main cluster sample. We see that the accretion rate has been fairly uniform over the past  $\sim 8$  Gyr, with the median lookback time to accretion at  $\sim 4-5$  Gyr. Interestingly, as shown by the red-dashed line, galaxies that were accreted as part of group-mass halos with  $M > 10^{13} h^{-1} M_\odot$  are biased to having been accreted later than the full sample. Specifically, the median lookback time for galaxies accreted as part of a group-mass system is  $\sim 3-4$  Gyr. This is not surprising, since it takes time for group-mass systems to form in a hierarchical universe. Indeed, we suspect that this fact is driving the double-peaked signature in the accretion time histogram, which has a slight dip at  $\sim 4$  Gyr. We do not find a trend between the accretion time distribution and cluster mass within our sample. Table 1 lists the median lookback accretion times for each cluster individually.

Another way to gain insight into the history of cluster galaxies is to quantify the amount of time a galaxy spends within a host halo of a given mass. Figure 7 shows the mean time that a cluster galaxy has spent in a host halo of a given mass, averaged over the history of the simulation. We see that this time-weighted host mass distribution for cluster galaxies is *bimodal* – on average, cluster galaxies have spent time either in their cluster or within a galaxy-mass halo prior to

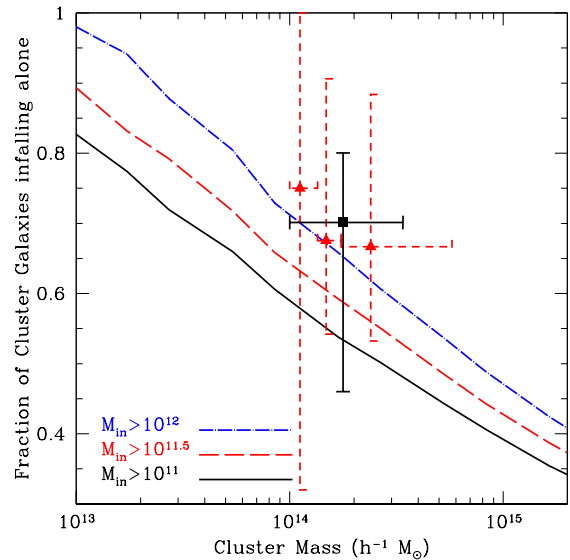


FIG. 5.— Fraction of surviving cluster galaxies that fell into the cluster without a bright companion in their host halo at the time of accretion. The three triangle data points are taken from our main sample of simulated, where galaxy halos are defined with  $M_{\text{in}} > 10^{11.5} h^{-1} M_\odot$ ,  $M_r \leq -18.5$ . The square data point is from our high-resolution sample,  $M_r \leq -16.4$ , with galaxies identified using our  $M_{\text{in}} > 10^{11} h^{-1} M_\odot$  criterion. Error bars along the y axis for the points reflect the 68 percentile range, and the error bars along the x-axis reflect the mass range of clusters included in the bin. The lines correspond to data generated by the semi-analytic substructure code of Zentner et al. (2005). The black (solid) line is for a sample of galaxies with  $M_{\text{in}} \geq 10^{11.0} h^{-1} M_\odot$  ( $M_r \lesssim -16.4$ ), the red (dashed) line is for our standard mass cuts of  $M_{\text{in}} \geq 10^{11.5} h^{-1} M_\odot$  ( $M_r \lesssim -18.5$ ), and the blue (dot-dashed) line is for a sample with  $M_{\text{in}} \geq 10^{12.0} h^{-1} M_\odot$ . Both the  $M_{\text{in}} > 10^{11.5}$  and  $M_{\text{in}} > 10^{12.0}$  samples have a criteria of  $M_{\text{cr}} \geq 10^{11.0} h^{-1} M_\odot$ . The  $M_{\text{in}} > 10^{11.0}$  sample matches our high resolution sample with  $M_{\text{cr}} \geq 2 \times 10^{10.0} h^{-1} M_\odot$ . Note that all three samples show the same trends. The only difference between them is that the trend is simply offset based on the mass of the sample.

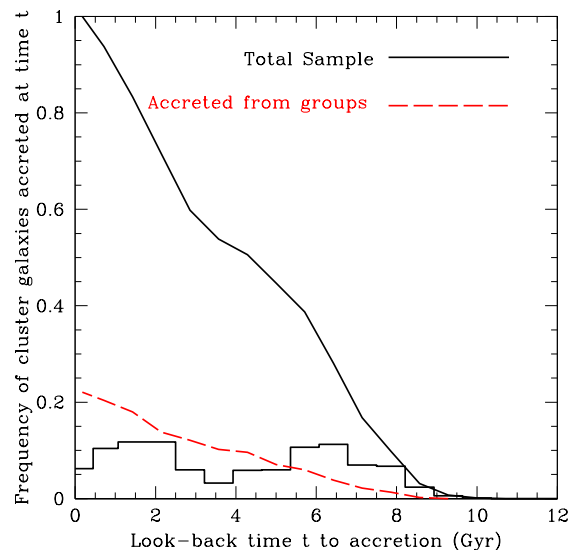


FIG. 6.— Differential and cumulative distributions of accretion times for our primary sample,  $M_r \leq -18.5$  of N-body cluster galaxies at  $z=0$ . The solid black line shows the distribution of the whole sample. The red long-dashed line shows the cumulative accretion times for the subset of cluster galaxies that were accreted from group-mass halos with  $M > 10^{13} h^{-1} M_\odot$ . Note that galaxies accreted from group halos are biased to fall into clusters later than other galaxies.

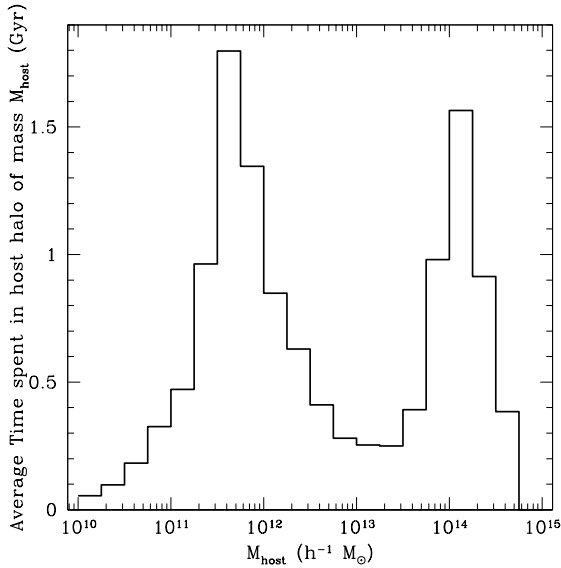


FIG. 7.— Average time that  $z = 0$  cluster galaxies (with  $M_{in} > 10^{11.5} h^{-1} M_{\odot}$ ,  $M_r \lesssim -18.5$ ) spend in host halos of mass  $M_{\text{host}}$ . Overall, cluster galaxies spend very little time in group-size of mass  $10^{12.5-13.5} h^{-1} M_{\odot}$ .

accretion. This distribution is calculated by examining the mass of each galaxy’s dark matter halo at each of the snapshots taken from the simulation. The simplifying assumption is made that the halo spends all of its time at that given mass until the next timestep. The pronounced dip in the middle shows that cluster galaxies tend to *avoid* spending time in groups. Here we have used the full sample of cluster galaxies with  $M_{in} > 10^{11.5} h^{-1} M_{\odot}$  to compute the average time that a cluster galaxy has spent in a host halo of a given mass. The peaks of the distribution are at the single galaxy-halo scale,  $\sim 10^{11.5} h^{-1} M_{\odot}$ , and at the median cluster scale  $\sim 10^{14.2} h^{-1} M_{\odot}$ . Note that galaxies can spend some time in halos smaller than our  $M_{in}$  threshold. Specifically, these halos grew from a small mass to a mass larger than  $10^{11.5} h^{-1} M_{\odot}$  before being accreted. It is clear that, on average, cluster galaxies spend very little time in the group-mass halos between  $10^{12.5}$  and  $10^{13.5} h^{-1} M_{\odot}$ .

Figure 8 makes a similar point, but in a more extreme fashion. Here we plot the fraction of galaxies that have spent any time within a halo within a given mass bin. We use the same simplifying assumption that the halo remains at the same mass until the next time step, therefore our ability to determine whether halos have spent anytime in a halo is limited by our output timestep spacing. In this figure, a value of unity implies that every galaxy has spent at least some time in a halo of this size.

### 3.4. Cluster Galaxies and Merger Histories

It is common to argue that spheroidal galaxies are associated with halos that have undergone significant mergers. This motivates us to compare the merger histories of field and cluster galaxies. The left panel of Figure 9 shows the cumulative fraction of cluster galaxies halos ( $M_{in} > 10^{11.5} h^{-1} M_{\odot}$ ,  $M_r \lesssim -18.5$ ) that have had a large merger since a given lookback time. The right panel shows the same statistic, now for *field* halos with  $M > 10^{11.5} h^{-1} M_{\odot}$ . The different line types correspond to different mass-ratio mergers:  $m/M_0 = 1/10$  to  $2/5$  from top (solid) to bottom (dashed). The mass ratio is defined to be the ratio relative to  $M_0 = M_{in}$  for cluster galaxies

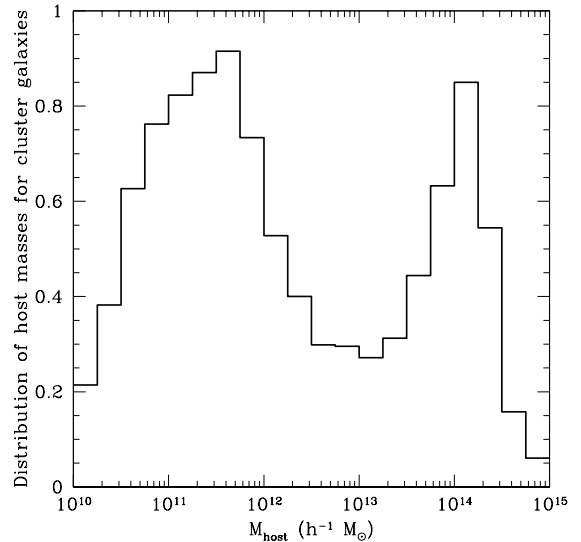


FIG. 8.— Fraction of  $z = 0$  cluster galaxies (with  $M_{in} > 10^{11.5} h^{-1} M_{\odot}$ ,  $M_r \lesssim -18.5$ ) that have spent *any* time in a host of mass  $M_{\text{host}}$ . We allow objects to appear in multiple mass bins as long as they have any time in a host halo of a given mass.

and relative to  $M_0 = M$  at  $z = 0$  for field halos.

At large lookback times cluster galaxies and field galaxies show similar results, at least for intermediate-size mergers. The total fraction of systems with  $> 1/10$  and  $> 1/5$  mergers in the last  $\sim 10$  Gyr are  $\sim 75\%$  and  $\sim 40\%$ , respectively, for both the cluster and field populations. The cluster population has a larger fraction of systems that have *ever* experienced *very* large mergers. For example,  $\sim 25\%$  of cluster galaxies have experienced something larger than a 0.3 merger in the last 10 Gyr, compared to just  $\sim 15\%$  in the field.

Perhaps the most striking difference is that the cluster population is much less likely to have had a *recent* ( $< 6$  Gyr) merger event than galaxies in the field. The fraction of cluster galaxies with a significant merger in the last  $\sim 6$  Gyr is less than  $\sim 5\%$ . Given that half of cluster galaxies were accreted more than  $\sim 4-5$  Gyr ago (Figure 6), this general result is not surprising. We expect the high-speed cluster environment to greatly reduce the likelihood for a merger. Large mergers are more likely to occur in the field.

## 4. DISCUSSION

### 4.1. Pre-processing

Galaxy groups provide an important intermediate environment between the field and high-density clusters for testing ideas about galaxy formation and evolution (Zabludoff & Mulchaey 1998). Indeed, it is possible that pre-processing in the group environment prior to the assembly of galaxy clusters is an important factor in explaining why cluster galaxies differ significantly from the field population. Assuming that  $\Lambda$ CDM provides an accurate description of the universe, the simulations presented here allow us to characterize the importance of groups in the global formation of galaxy clusters.

Note that with our definition, groups and clusters are defined using the standard “virial” over-density boundary for host dark matter halos. In this case, most galaxies in the universe *do not* reside in groups.  $\Lambda$ CDM simulations suggest that only  $\sim 10\%$  of  $\sim L_*$  galaxy halos reside within the virial radii of group or cluster halos (e.g., Berrier et al. 2006, and refer-

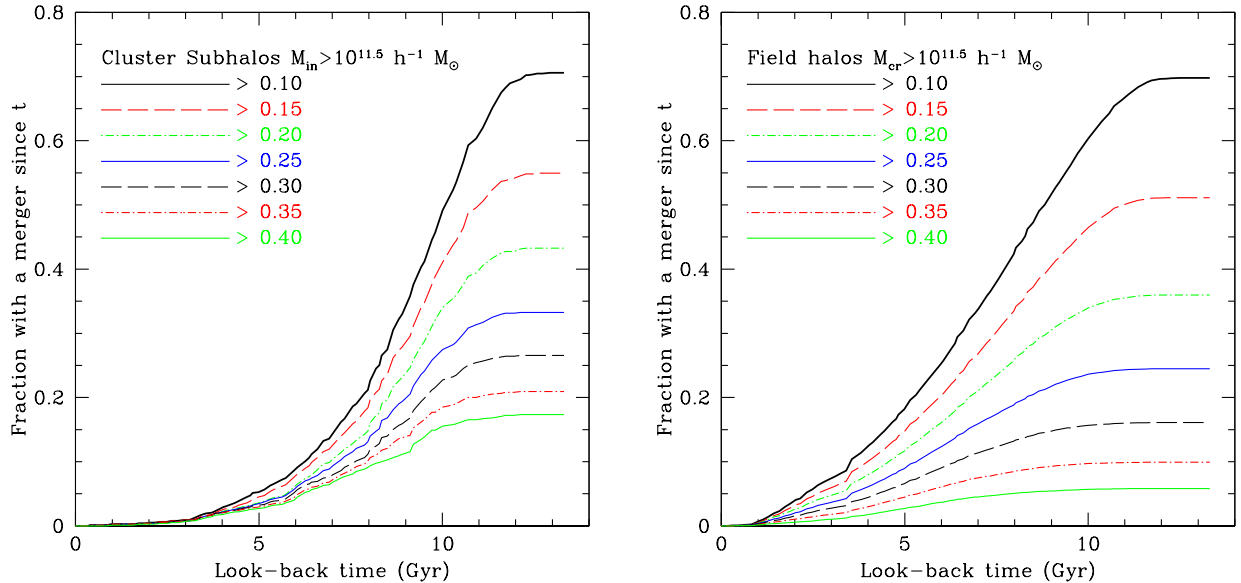


FIG. 9.— Fraction of galaxy halos that have undergone a merger larger than a listed fraction within a given look-back time. The *left panel* is restricted to our sample of cluster galaxies with  $M_{in} > 10^{11.5} h^{-1} M_{\odot}$  and the *right panel* includes all field halos with  $z = 0$  masses larger than  $10^{11.5} h^{-1} M_{\odot}$ . The labeled line types correspond to different merger ratio fractions,  $M/M_0$ , where  $M$  is the mass of the merging object and  $M_0$  is the mass of the galaxy halo, with  $M_0 = M_{in}$  for cluster galaxies and  $M_0 = M$  at  $z = 0$  for field halos.

ences therein). It is interesting then to ask whether majority of *cluster* galaxies were assembled from the field population or whether they are biased to be galaxies that evolved in groups.

While Figure 1 demonstrates that a significant fraction of the *mass* in clusters is accreted from group-size dark matter halos, Figures 2 and 3 show that the same is not true for *galaxies* in clusters. Less than 17% of cluster galaxies in  $\sim 10^{14.2} h^{-1} M_{\odot}$  clusters fell in as a part of a group with five or more other galaxies. Similarly,  $\sim 25\%$  were accreted as part of a halo more massive than  $10^{13} h^{-1} M_{\odot}$ . This finding suggests that pre-processing cannot play the dominant role in differentiating cluster galaxy populations from the field. As we discuss below, our results suggest that global differences between cluster and field populations must be set by environmental influences associated with the clusters themselves.

It is also important to emphasize that the pre-cluster evolution histories of cluster galaxies varies significantly from cluster to cluster. This variation is demonstrated in Figure 4. For example, while most of our clusters ( $44/53 \simeq 83\%$ ) have galaxy populations that are completely devoid of objects that were accreted from groups with five or more companions, a small fraction ( $4/53 \simeq 7.5\%$ ) of our clusters have a majority ( $f > 0.5$ ) of their galaxies that fell into the cluster from groups of this kind.

Zabludoff & Mulchaey (1998) have suggested that cD galaxies in clusters may form originally in the group environment. Our results do not prevent such a scenario from occurring in some cases, particularly in those where a large group-scale merger has occurred recently. As seen in Figures 7 and 8, there are always a few galaxies that evolve in groups. Additionally, these figures only include galaxies that survive to the present. Galaxies that are accreted into the cluster and destroyed may provide material for the growth of cD galaxies and is consistent with the results of Lin & Mohr (2004).

We also find a weak trend between the fraction of cluster galaxies that could have experienced pre-processing and the mass of the cluster. For the lowest mass third of our

cluster sample,  $M_{clus} \simeq 10^{14.05} h^{-1} M_{\odot}$ , we see from Figure 5 that  $\sim 75\%$  of cluster galaxies are accreted directly from the field. This number drops to  $\sim 65\%$  in our largest mass sample,  $M_{clus} \simeq 10^{14.35} h^{-1} M_{\odot}$ . This trend with mass is certainly real, however, the variation from cluster-to-cluster is much stronger than the mass trend itself. The results of Weinmann et al. (2006) suggest that the early-type fraction of cluster galaxies rises from  $\sim 50\%$  to  $\sim 55\%$  in clusters of mass  $\sim 10^{14}$  to  $10^{14.5} h^{-1} M_{\odot}$ . It is possible that pre-processing could play a role in driving this weak mass trend.

#### 4.2. Cluster Galaxy Merger Histories

As we showed in Figure 9, there are clear statistical differences between the merger histories of cluster galaxies and field galaxy halos. Nonetheless, it is unlikely that merger histories alone can explain the morphology, color, and spectral-type differences seen between cluster galaxies and the field. For example, let us take 60% and 30% as characteristic bulge-dominated fractions in clusters (within  $< R_{vir}$ ) and the field, respectively (Whitmore & Gilmore 1991; Postman et al. 2005). By examining Figure 9 we see that the field spheroid population potentially could be associated directly with the  $\sim 30\%$  of field halos that have experienced a  $> 1/5$  merger in the last  $\sim 9$  Gyr. However, the 60% cluster spheroid population cannot be explained with the same set of assumptions: only  $\sim 25\%$  of cluster halos have had a similar merger in the same period of time, and only  $\sim 45\%$  have *ever* experienced a  $> 1/5$  merger.

Given that merger histories alone cannot explain the differences between cluster and field populations, we are forced to construct more complicated scenarios involving mergers to help explain the observed population differences. For example, galaxies in the field are expected to be surrounded by reservoirs of baryons that can cool to reform a disk after a large merger. Galaxies in clusters would likely be stripped of this reservoir by the ambient cluster medium, making it impossible for cluster galaxies to accrete material to reform a disk after they have fallen into the cluster. The right panel of

Figure 9 shows that we could potentially associate the  $\sim 30\%$  of bulge-dominated galaxies in the field with the  $\sim 1/10$  mergers that occurred within the last  $\sim 6$  Gyr (and assume that merger remnants, older than 6 Gyr, in the field have reformed disks). However, even this scenario would have difficulties explaining the cluster population: only  $\sim 70\%$  of cluster galaxies have *ever* experienced a  $> 1/10$  merger (left panel, Figure 9) and only  $\sim 35\%$  were accreted into the cluster in the last 6 Gyr. Thus, obtaining more than a  $\sim 25\%$  spheroid fraction without other transformational effects (i.e., harassment) would seem difficult.

The scenario discussed above is similar to that adopted in many semi-analytic models (e.g., Benson et al. 2001; Springel et al. 2001), where galaxies experience “strangulation” as their fresh gas supply is cut off when they fall into the cluster environment. Not only does this effect prevent the possible reformation of disks, but it can cause the galaxy to redden over  $\sim 1-3$  Gyr timescales (Poggianti et al. 1999; Balogh et al. 2000; Ellingson et al. 2001) and thus help explain the morphological *and* spectral mix of cluster populations. It should be noted, however, that observations of moderate redshift clusters suggest that either two different physical processes or at least two different timescales are responsible for spectral and morphological transformations in clusters (Poggianti et al. 1999).

#### 4.3. Accretion Times and Galaxy Transformation

The timescales available for cluster galaxy transformation can be garnered directly from Figure 6 (also Figure 7). We expect gravitational processes like harassment to operate over timescales similar to the cluster dynamical time,  $1/\sqrt{G\rho_{\text{vir}}} \simeq 4$  Gyr. Given this, Figure 6 shows that  $\sim 70\%$  of cluster galaxies have been in the cluster potential long enough to experience significant dynamical perturbations. In order to transform a  $\sim 70\%$  field disk population to a  $\sim 40\%$  cluster disk population, we need  $\sim 3/7 \simeq 40\%$  of accreted galaxies to be affected (assuming spheroids remain spheroids). Figure 6 shows that  $\sim 40\%$  of cluster galaxies have been within the cluster longer than  $\sim 6$  Gyr ( $\sim 1.5$  dynamical times). This estimate suggests that  $\sim 6$  Gyr is a typical transformation timescale for cluster galaxies.

The timescale for strangulation is much shorter than a dynamical time, and should begin to operate as soon as the galaxy encounters the intra-cluster medium ( $\lesssim 1$  Gyr). We expect ram pressure to be important at higher hot gas densities than strangulation (i.e., at smaller cluster-centric radii) and therefore the associated timescale for ram pressure to act should be somewhat longer than that for strangulation, perhaps of order a dynamical time. Given the infall time distribution in Figure 6, we expect that most cluster galaxies will have been affected to some degree by the cutoff of fresh gas infall (e.g.,  $\sim 90\%$  with infall times  $> 1$  Gyr). This process can alter spectral properties without affecting the morphological mix. A smaller fraction have been in the cluster for  $\sim 1$  dynamical time ( $\sim 50\%$  with infall times  $> 4$  Gyr) – long enough to experience significant dynamical (morphological) transformations.

The above discussions provide some qualitative evaluation of ideas that may explain why the cluster galaxy population is different from the field population. A similar analysis, involving a more precise characterization of radial dependencies and merger histories, and the evolution of cluster galaxy infall times with the redshift of the cluster, will be an important avenue for future investigation.

## 5. CONCLUSIONS

We use two cosmological N-body simulations set within the concordance  $\Lambda$ CDM cosmology to study the formation of cluster-sized dark matter halos with masses spanning  $M_{\text{clus}} = 10^{14.0-14.76} h^{-1} M_{\odot}$ . Our primary results are based on tracking the merger histories of galaxy subhalos within these clusters. These, our cluster galaxies, are picked to have masses  $M_{\text{in}} > 10^{11.5} h^{-1} M_{\odot}$  at the time they first fell into their host halos, and should correspond approximately to  $\sim 0.1 L_*$  galaxies. Our conclusions may be summarized as follows.

- We find that the majority of cluster galaxies ( $\sim 70\%$ ) are accreted directly from the field, as the only objects within their dark matter halos at the time of their infall into the cluster virial radius. A minority ( $\sim 25\%$ ) were accreted as part of  $M > 10^{13} h^{-1} M_{\odot}$  group-mass halos, and a small fraction ( $\sim 12\%$ ) of cluster galaxies fell into their clusters with more than 5 galaxies in their halos at the time of accretion.
- Cluster galaxy infall histories show significant variation from cluster to cluster. For example, 9/53 ( $\sim 17\%$ ) of the clusters in our sample were assembled *entirely* from the accretion of field galaxies. However, 4/53 ( $\sim 7\%$ ) of our clusters had a *majority* of their galaxies ( $f > 0.5$ ) accreted from groups with five or more companions. Therefore, while on average cluster galaxies tend to be accreted from the field, there are some clusters that do not follow this trend.
- More massive clusters have a smaller fraction of their galaxies (at fixed luminosity) accreted directly from the field. Approximately 75% of  $\sim 0.1 L_*$  galaxies in  $M \simeq 10^{14} h^{-1} M_{\odot}$  halos are accreted from the field, compared to  $\sim 65\%$  of galaxies in  $M \simeq 10^{14.35} h^{-1} M_{\odot}$  clusters. The scatter in formation histories from cluster-to-cluster at fixed mass is more significant than this mass trend.
- The median lookback time to accretion for galaxies within clusters is  $\sim 4.5$  Gyr, and  $\sim 85\%$  of galaxies are accreted between 1 and 9 Gyr ago. By assuming that cluster galaxies are accreted with a morphological mix similar to the field, we estimate an approximate cluster-environmental transformation timescale of  $\sim 6$  Gyr.
- Galaxy subhalos in clusters are significantly less likely to have had a recent ( $\lesssim 6$  Gyr) merger than similar mass galaxy halos in the field. The merger fraction within the past  $\sim 12$  Gyr is  $\sim 5\%$  higher for the cluster subhalo population.

Taken together, these results suggest that the observed population differences between galaxies in clusters and those in the field are driven primarily by internal cluster processes. Given  $\Lambda$ CDM as a basis, merging in the group environment, or any other type of pre-processing in galaxy groups prior to cluster assembly, cannot be a major factor in setting the nearly two-to-one difference in early-type fraction between clusters and the field.

Approximately half of an average cluster’s population is accreted more than 4 Gyr ago ( $\sim 1$  dynamical time). This allows ample time for gravitational processes to drive morphological



transformations within the cluster environment. Moreover, interactions with the intra-cluster medium that remove gas and suppress star formation in cluster galaxies likely begin to operate on even shorter timescales ( $\sim 1$  Gyr). Therefore, most cluster galaxies ( $\sim 90\%$ ) will be affected by the cluster environment, at least to some degree.

While our results suggest that pre-processing is not the dominant mechanism in setting galaxy cluster processes, we do find most clusters have a non-negligible fraction of their galaxies accreted from a group environment. This is especially true for the more massive clusters in our sample ( $\sim 10^{14.35} h^{-1} M_{\odot}$ ), for which we find that  $\sim 28\%$  of their galaxies were accreted as part of a halo larger than a group-mass scale  $M > 10^{13} h^{-1} M_{\odot}$ . Therefore, some amount of preprocessing should occur.

As mentioned in the introduction, important constraints on the types of processes that act to shape the cluster and group galaxy populations come from studies at intermediate to high redshift (Butcher & Oemler 1978; Tran et al. 2005; Gerke et al. 2007; Capak et al. 2007; Finn et al. 2008). A

valuable direction of future work will be to combine the predicted N-body statistics for cluster halo assembly time with these results as a means to constrain specific scenarios for galaxy transformation and star formation suppression.

The simulations were run on the Seaborg machine at Lawrence Berkeley National Laboratory (Project PI: Joel Primack). We thank Anatoly Klypin for running the simulation and making it available to us. We acknowledge Andrew Zentner for the use of his semi-analytic substructure code and for useful comments on the manuscript. We thank Alison Coil, Jeff Cooke, Asantha Cooray, Alan Dressler, Margaret Geller, Manoj Kaplinghat, Andrey Kravtsov, Jeremy Tinker, and Frank van den Bosch for useful conversations. JCB and JSB are supported by NSF grant AST-0507916; JCB, JSB, and EJB are supported by the Center for Cosmology at UC Irvine. RHW received support from the U.S. Department of Energy under contract number DE-AC02-76SF00515.

## REFERENCES

- Allgood, B., Flores, R. A., Primack, J. R., Kravtsov, A. V., Wechsler, R. H., Faltenbacher, A., & Bullock, J. S. 2006, *MNRAS*, 367, 1781
- Balogh, M. L., Baldry, I. K., Nichol, R., Miller, C., Bower, R., & Glazebrook, K. 2004, *ApJ*, 615, L101
- Balogh, M. L., Navarro, J. F., & Morris, S. L. 2000, *ApJ*, 540, 113
- Benson, A. J., Frenk, C. S., Baugh, C. M., Cole, S., & Lacey, C. G. 2001, *MNRAS*, 327, 1041
- Berrier, J. C., Bullock, J. S., Barton, E. J., Guenther, H. D., Zentner, A. R., & Wechsler, R. H. 2006, *ApJ*, 652, 56
- Blanton, M. R., Hogg, D. W., Bahcall, N. A., Brinkmann, J., Britton, M., Connolly, A. J., Csabai, I., Fukugita, M., Loveday, J., Meiksin, A., Munn, J. A., Nichol, R. C., Okamura, S., Quinn, T., Schneider, D. P., Shimasaku, K., Strauss, M. A., Tegmark, M., Vogeley, M. S., & Weinberg, D. H. 2003, *ApJ*, 592, 819
- Bryan, G. L. & Norman, M. L. 1998, *ApJ*, 495, 80
- Butcher, H. & Oemler, Jr., A. 1978, *ApJ*, 219, 18
- Capak, P., Abraham, R. G., Ellis, R. S., Mobasher, B., Scoville, N., Sheth, K., & Koekemoer, A. 2007, *ApJS*, 172, 284
- Chung, A., van Gorkom, J. H., Kenney, J. D. P., & Vollmer, B. 2007, *ApJ*, 659, L115
- Coil, A. L., Newman, J. A., Croton, D., Cooper, M. C., Davis, M., Faber, S. M., Gerke, B. F., Koo, D. C., Padmanabhan, N., Wechsler, R. H., & Weiner, B. J. 2008, *ApJ*, 672, 153
- Conroy, C., Wechsler, R. H., & Kravtsov, A. V. 2006, *ApJ*, 647, 201
- Diaferio, A., Kauffmann, G., Balogh, M. L., White, S. D. M., Schade, D., & Ellingson, E. 2001, *MNRAS*, 323, 999
- Dressler, A. 1980, *ApJ*, 236, 351
- Dressler, A., Oemler, A. J., Couch, W. J., Smail, I., Ellis, R. S., Barger, A., Butcher, H., Poggianti, B. M., & Sharples, R. M. 1997, *ApJ*, 490, 577
- Ellingson, E., Lin, H., Yee, H. K. C., & Carlberg, R. G. 2001, *ApJ*, 547, 609
- Finn, R. A., Balogh, M. L., Zaritsky, D., Miller, C. J., & Nichol, R. C. 2008, *ArXiv:802.2282 [astro-ph]*
- Gerke, B. F., Newman, J. A., Faber, S. M., Cooper, M. C., Croton, D. J., Davis, M., Willmer, C. N. A., Yan, R., Coil, A. L., Guhathakurta, P., Koo, D. C., & Weiner, B. J. 2007, *MNRAS*, 376, 1425
- Gunn, J. E. & Gott, J. R. I. 1972, *ApJ*, 176, 1
- Kauffmann, G., White, S. D. M., & Guiderdoni, B. 1993, *MNRAS*, 264, 201
- Klypin, A., Gottlöber, S., Kravtsov, A. V., & Khokhlov, A. M. 1999, *ApJ*, 516, 530
- Kravtsov, A. V., Gnedin, O. Y., & Klypin, A. A. 2004, *ApJ*, 609, 482
- Kravtsov, A. V., Klypin, A. A., & Khokhlov, A. M. 1997, *ApJS*, 111, 73
- Larson, R. B., Tinsley, B. M., & Caldwell, C. N. 1980, *ApJ*, 237, 692
- Lin, Y.-T. & Mohr, J. J. 2004, *ApJ*, 617, 879
- Loh, Y., Ellingson, E., Yee, H. K. C., Gilbank, D. G., Gladders, M. D., & Barrientos, L. F. 2008, *ArXiv:802.3726 [astro-ph]*
- Moore, B., Katz, N., Lake, G., Dressler, A., & Oemler, A. 1996, *Nature*, 379, 613
- Oemler, A. J. 1974, *ApJ*, 194, 1
- Okamoto, T. & Nagashima, M. 2001, *ApJ*, 547, 109
- Poggianti, B. M., Smail, I., Dressler, A., Couch, W. J., Barger, A. J., Butcher, H., Ellis, R. S., & Oemler, A. J. 1999, *ApJ*, 518, 576
- Poggianti, B. M., von der Linden, A., De Lucia, G., Desai, V., Simard, L., Halliday, C., Aragón-Salamanca, A., Bower, R., Varela, J., Best, P., Clowe, D. I., Dalcanton, J., Jablonka, P., Milvang-Jensen, B., Pello, R., Rudnick, G., Saglia, R., White, S. D. M., & Zaritsky, D. 2006, *ApJ*, 642, 188
- Postman, M., Franx, M., Cross, N. J. G., Holden, B., Ford, H. C., Illingworth, G. D., Goto, T., Demarco, R., Rosati, P., Blakeslee, J. P., Tran, K.-V., Benítez, N., Clampin, M., Hartig, G. F., Homeier, N., Ardila, D. R., Bartko, F., Bouwens, R. J., Bradley, L. D., Broadhurst, T. J., Brown, R. A., Burrows, C. J., Cheng, E. S., Feldman, P. D., Golimowski, D. A., Gronwall, C., Infante, L., Kimble, R. A., Krist, J. E., Lesser, M. P., Martel, A. R., Mei, S., Menanteau, F., Meurer, G. R., Miley, G. K., Motta, V., Sirianni, M., Sparks, W. B., Tran, H. D., Tsvetanov, Z. I., White, R. L., & Zheng, W. 2005, *ApJ*, 623, 721
- Postman, M. & Geller, M. J. 1984, *ApJ*, 281, 95
- Purcell, C. W., Bullock, J. S., & Zentner, A. R. 2007, *ApJ*, 666, 20
- Quilis, V., Moore, B., & Bower, R. 2000, *Science*, 288, 1617
- Somerville, R. S. & Kolatt, T. S. 1999, *MNRAS*, 305, 1
- Springel, V., White, S. D. M., Tormen, G., & Kauffmann, G. 2001, *MNRAS*, 328, 726
- Stewart, K. R., Bullock, J. S., Wechsler, R. H., Maller, A. H., & Zentner, A. R. 2008, *ApJ*, accepted, *ArXiv:711.5027 [astro-ph]*
- Tonnesen, S. 2007, *New Astronomy Review*, 51, 80
- Toomre, A. & Toomre, J. 1972, *ApJ*, 178, 623
- Tran, K.-V. H., Simard, L., Zabludoff, A. I., & Mulchaey, J. S. 2001, *ApJ*, 549, 172
- Tran, K.-V. H., van Dokkum, P., Illingworth, G. D., Kelson, D., Gonzalez, A., & Franx, M. 2005, *ApJ*, 619, 134
- Treu, T., Ellis, R. S., Kneib, J.-P., Dressler, A., Smail, I., Czoske, O., Oemler, A., & Natarajan, P. 2003, *ApJ*, 591, 53
- Wang, L., Li, C., Kauffmann, G., & De Lucia, G. 2006, *MNRAS*, 371, 537
- Wechsler, R. H., Zentner, A. R., Bullock, J. S., Kravtsov, A. V., & Allgood, B. 2006, *ApJ*, 652, 71
- Weinmann, S. M., van den Bosch, F. C., Yang, X., & Mo, H. J. 2006, *MNRAS*, 366, 2
- Whitmore, B. C. & Gilmore, D. M. 1991, *ApJ*, 367, 64
- Zabludoff, A. 2002, in *Astronomical Society of the Pacific Conference Series*, Vol. 257, *AMiBA 2001: High-Z Clusters, Missing Baryons, and CMB Polarization*, ed. L.-W. Chen, C.-P. Ma, K.-W. Ng, & U.-L. Pen, 123–+
- Zabludoff, A. I. & Mulchaey, J. S. 1998, *ApJ*, 496, 39
- Zentner, A. R. 2007, *International Journal of Modern Physics D*, 16, 763
- Zentner, A. R., Berlind, A. A., Bullock, J. S., Kravtsov, A. V., & Wechsler, R. H. 2005, *ApJ*, 624, 505
- Zentner, A. R. & Bullock, J. S. 2003, *ApJ*, 598, 49

TABLE 1  
CLUSTER HALO PROPERTIES

Cluster id	$M_{\text{clus}}$ ( $10^{14} h^{-1} M_{\odot}$ )	$R_{\text{vir}}$ ( $h^{-1} \text{Mpc}$ )	$N_{\text{grp}}/N_{\text{total}}$ ( $> 10^{11.5}$ )	$N_0/N_{\text{total}}$ ( $> 10^{11.5}$ )	$N_{\geq 5}/N_{\text{total}}$ ( $> 10^{11.5}$ )	$T_{1/2}$ Mass Gyr	$T_{1/2}$ Galaxies Gyr	$N_{\text{grp}}/N_{\text{total}}$ ( $> 10^{11.0}$ )
1.120	5.86	1.71	15/53	34/53	6/53	7.1	2.4	NA
2.120	4.41	1.56	10/31	23/31	0/31	7.4	5.0	NA
3.120	3.80	1.48	3/23	19/23	0/23	7.4	4.9	NA
1.80	3.44	1.44	6/28	17/28	0/28	6.2	5.2	26/102
4.120	2.95	1.36	9/23	18/23	0/23	4.9	2.2	NA
5.120	2.77	1.34	5/26	14/26	0/26	5.2	5.8	NA
6.120	2.60	1.31	7/33	21/33	0/33	5.2	5.5	NA
7.120	2.57	1.30	7/21	14/21	0/21	3.4	1.8	NA
2.80	2.44	1.28	0/19	19/19	0/19	7.8	6.5	6/89
3.80	2.11	1.22	3/19	17/19	0/19	6.2	3.0	11/51
8.120	2.06	1.21	4/23	9/23	10/23	8.4	6.1	NA
9.120	1.94	1.19	23/41	21/41	9/41	6.6	4.5	NA
10.120	1.92	1.18	8/27	16/27	0/27	4.7	3.0	NA
11.120	1.88	1.17	6/22	18/22	0/22	8.1	5.8	NA
4.80	1.87	1.17	6/19	13/19	5/19	5.8	4.9	25/71
12.120	1.85	1.17	2/19	17/19	0/19	6.0	5.5	NA
13.120	1.80	1.16	2/17	15/17	0/17	5.8	4.5	NA
14.120	1.74	1.14	12/16	9/16	7/16	0.7	1.3	NA
15.120	1.71	1.14	0/17	17/17	0/17	8.7	5.7	NA
16.120	1.60	1.11	6/16	9/16	0/16	7.4	2.1	NA
17.120	1.59	1.11	7/15	8/15	0/15	2.4	3.0	NA
5.80	1.55	1.10	0/18	14/18	0/18	7.4	3.0	3/43
6.80	1.51	1.09	3/15	10/15	5/15	6.2	3.0	9/47
18.120	1.51	1.09	5/13	9/13	0/13	2.2	2.2	NA
19.120	1.49	1.09	0/10	10/10	0/10	6.5	7.1	NA
7.80	1.48	1.08	6/23	16/23	0/23	6.2	3.9	14/67
20.120	1.48	1.08	1/11	6/11	0/11	5.8	4.2	NA
21.120	1.48	1.08	3/8	7/8	0/8	3.6	1.8	NA
22.120	1.48	1.08	1/6	4/6	0/6	7.6	1.9	NA
23.120	1.45	1.08	1/10	8/10	0/10	7.3	2.1	NA
8.80	1.44	1.07	3/10	5/10	0/10	6.8	5.2	9/42
9.80	1.42	1.07	1/9	8/9	0/9	5.5	3.9	9/37
24.120	1.41	1.07	0/11	9/11	0/11	7.6	4.9	NA
25.120	1.39	1.06	3/12	8/12	0/12	7.4	7.1	NA
26.120	1.39	1.06	1/7	5/7	0/7	6.8	6.0	NA
27.120	1.34	1.05	3/13	0/13	13/13	5.5	5.8	NA
28.120	1.28	1.03	1/5	5/5	0/5	6.9	3.9	NA
29.120	1.27	1.03	0/12	10/12	0/12	6.0	5.0	NA
30.120	1.23	1.02	0/9	9/9	0/9	7.1	6.8	NA
31.120	1.23	1.02	3/15	8/15	0/15	6.6	2.4	NA
32.120	1.22	1.02	0/10	10/10	0/10	7.1	4.1	NA
33.120	1.16	1.00	0/8	6/8	0/8	7.4	5.3	NA
10.80	1.14	0.99	2/8	6/8	0/8	7.8	6.5	3/30
11.80	1.12	0.99	0/12	12/12	0/12	7.4	6.2	0/30
34.120	1.12	0.99	1/5	4/5	0/5	6.1	5.8	NA
35.120	1.12	0.99	1/7	6/7	0/7	5.8	1.8	NA
36.120	1.12	0.99	0/8	6/8	0/8	5.8	2.2	NA
37.120	1.10	0.98	0/12	5/12	7/12	5.2	4.4	NA
38.120	1.09	0.98	3/9	4/9	0/9	7.3	3.6	NA
39.120	1.08	0.98	4/9	2/9	7/9	8.4	0.7	NA
12.80	1.01	0.95	0/9	9/9	0/9	8.1	3.9	0/34
40.120	1.01	0.95	0/6	2/6	0/6	7.1	6.1	NA
41.120	1.01	0.95	0/9	9/9	0/9	8.5	4.7	NA

Note – The first column denotes the our id numbers, ordered by mass within their respective simulation box. The number following the decimal point corresponds to the box size in comoving  $h^{-1} \text{Mpc}$ . The second column lists the cluster virial mass in units of  $10^{14} h^{-1} M_{\odot}$ . The third column lists the cluster virial radius in  $h^{-1} \text{Mpc}$ . The fourth column,  $N_{\text{grp}}/N_{\text{total}}$ , lists the fraction of ( $M_{\text{in}} > 10^{11.5} h^{-1} M_{\odot}$ ) galaxies that were accreted in a group-size halos with  $M > 10^{13} h^{-1} M_{\odot}$ . The fifth and sixth columns list the fraction of galaxies that were accreted as the only object in their halo ( $N_0/N_{\text{total}}$ ) and with five or more companions in their halo ( $N_{\geq 5}/N_{\text{total}}$ ), respectively. Columns seven and eight show the approximate lookback times to the host halos accretion of half of its mass and half of its surviving substructure respectively. Finally, the last column is the same as the fourth column, except now we track the fraction of galaxies accreted in group-mass halos using our high-resolution sample of  $M_{\text{in}} > 10^{11} h^{-1} M_{\odot}$  galaxies.